Optics Letters

Dependence of quality factor on surface roughness in crystalline whispering-gallery mode resonators

Guoping Lin,[1,2] Rémi Henriet,[1] Aurélien Coillet,[1,3] Maxime Jacquot,[1] Luca Furfaro,[1] Gilles Cibiel,[4] Laurent Larger,[1] and Yanne K. Chembo[1,5,*]

[1]FEMTO-ST Institute, Univ. Bourgogne Franche-Comté, CNRS, Optics Department, 15B Avenue des Montboucons, 25030 Besançon cedex, France
[2]Currently at MOE Key Laboratory of Fundamental Quantities Measurement, School of Physics, Huazhong University of Science and Technology, Wuhan 430074, China
[3]Currently at Laboratoire Interdisciplinaire Carnot Bourgogne [CNRS UMR6303], Univ. Bourgogne-Franche-Comté, 9 Avenue A. Savary, 21078 Dijon, France
[4]Centre National d'Etudes Spatiales (CNES), 18 Avenue Edouard Belin, F-31401 Toulouse, France
[5]GeorgiaTech-CNRS Joint International Laboratory [UMI 2958], Atlanta Mirror Site, School of Electrical and Computer Engineering, 777 Atlantic Dr NW, Atlanta, Georgia 30332, USA
*Corresponding author: yanne.chembo@femto-st.fr

Received 31 October 2017; revised 28 December 2017; accepted 29 December 2017; posted 2 January 2018 (Doc. ID 312430); published 25 January 2018

We present an experimental study of the variation of quality factor (Q-factor) of WGM resonators as a function of surface roughness. We consider mm-size whispering-gallery mode resonators manufactured with fluoride crystals, featuring Q-factors of the order of 1 billion at 1550 nm. The experimental procedure consists of repeated polishing steps, after which the surface roughness is evaluated using profilometry by white-light phase-shifting interferometry, while the Q-factors are determined using the cavity-ring-down method. This protocol permits us to establish an explicit curve linking the Q-factor of the disk-resonator to the surface roughness of the rim. We have performed measurements with four different crystals, namely, magnesium, calcium, strontium, and lithium fluoride. We have thereby found that the variations of Q-factor as a function of surface roughness is universal, in the sense that it is globally independent of the bulk material under consideration. We also discuss our experimental results in the light of theoretical estimates of surface scattering Q-factors already published in the literature.

OCIS codes: (120.3180) Interferometry; (140.4780) Optical resonators; (240.5450) Polishing; (240.5770) Roughness.

https://doi.org/10.1364/OL.43.000495

One of the key parameters for optical resonators is their quality factor (or Q-factor), which directly reflects their capacity to store photons at a given frequency. The simple relationship $Q = \omega_0 \tau_{ph}$, where ω_0 is the angular frequency of the photon and τ_{ph} the photon lifetime, indicates that Q-factors of the order of a billion are needed to store near-infrared photons ($\lambda_0 \sim 1550$ nm or $\omega_0/2\pi \sim 200$ THz) in the microsecond timescale.

For various fundamental research and technology developments, ultrahigh Q-factors ($Q > 10^8$) are therefore highly desired. From this perspective, whispering-gallery mode resonators (WGMR), which confine light by total internal reflections, are of particularly high interest for many technological applications [1,2]. In such resonators, light is able to travel circularly along the circumference of a compact and axisymmetrical monolithic geometry with very low losses. To date, the highest Q-factor reported from a passive WGMR is 3×10^{11} [3]. Recently, Q-factors above 10^{12} corresponding to photon lifetime in the millisecond timescale were also demonstrated in erbium-doped fluoride glass WGMR [4].

Benefiting from ultrahigh Q-factors and small mode volumes, WGMRs have become ideal platforms for exploring various applications [1,2,5], e.g., low threshold lasers have been produced using rare-earth-doped glass WGMRs [6], second-order nonlinear effects such as second-harmonic generation and optical parametric oscillation have been exploited in WGMRs made from nonlinear crystals such as lithium niobate ($LiNbO_3$) [7–10], beta barium borate (BBO) [11,12], lithium tetraborate ($Li_2B_4O_7$) [13], and silver gallium selenide ($AgGaSe_2$) [14]. As for the third-order nonlinearity, host material of WGMRs can be extended to centrosymmetric optical materials, especially fused silica [15], fused quartz [16], and fluoride crystals [17–25]. It should be noted that universal nonlinear scattering involving simultaneous Raman, Kerr, and Brillouin effects can also be simultaneously observed in such resonators [26]. Other applications of mm-size WGM resonators include sensors [27–30], gyroscopes [31,32], quantum optics [33], and many microwave photonics applications in the linear regime [34,35].

To fabricate such ultrahigh-Q WGMRs, one has to consider the loss mechanisms that limit the intrinsic Q-factors. Regarding WGMRs with no surface contamination or deformation, three

types of losses are typically taken into consideration: bulk material absorption (Q_{mat}), radiation (Q_{rad}), and surface scattering losses (Q_{ss}). The total Q-factor of the resonator can then be calculated as $Q^{-1} = Q_{mat}^{-1} + Q_{rad}^{-1} + Q_{ss}^{-1}$. However, in the cases of large (mm-size) WGMRs made with highly pure optical materials, we practically have $Q_{mat} > 10^{12}$ and $Q_{rad} \to +\infty$. Therefore, because these resonators typically feature a billion Q-factors, we are led to consider that $Q \to Q_{ss}$ and to infer that the main obstacle for achieving ultrahigh Q-factors is then linked to the scattering induced by the surface roughness of the WGMRs.

Theoretically, several expressions for estimating the surface scattering Q-factor Q_{ss} based on the surface roughness profiles of the WGMRs have been developed and updated (see for example [36–40]). Experimental efforts were made for investigating the validity of the formula developed in 1998 by Vernooy *et al.*, in which small fused-silica microspheres with a diameter of a few hundred micrometers were studied using an atomic force microscope (AFM) [38]. However, the validity of the theoretical estimations has not yet been quantitatively investigated for millimeter scale resonators, despite the critical importance of such resonators for a broad variety of technological applications (see for example [41]). Bridging this gap is the main objective of the present Letter.

We have fabricated several WGMRs with a diameter around 12 mm from different fluoride crystals, including magnesium fluoride (MgF_2), calcium fluoride (CaF_2), strontium fluoride (SrF_2), and lithium fluoride (LiF) (from Korth Kristalle GmbH). We have used the grinding and polishing method that was extensively presented in [42]. At every step of the polishing process, we measured the surface roughness and the maximum Q-factor of the disk resonator. As we progressed in the polishing procedure, the surface roughness decreased, and the Q-factors increased accordingly. The root-mean-square (rms) surface roughness σ was acquired using a homemade surface profilometer based on white-light phase-shifting interferometry [43–46]. This optical contactless profilometer, which is based on a Mirau-type interferometer microscope and the analysis of the white-light interference phase, is presented in Fig. 1. The Q-factors of these resonators at 1550 nm were obtained using the cavity-ring-down method [47], with the experimental setup presented in Fig. 2. The coupling between the scanning laser and the resonator was achieved using fiber tapers obtained by heating and pulling a standard single-mode fiber.

Figures 3(a)–3(c) show the reconstructed surface profiles using our homemade profilometer for WGM resonators made of MgF_2, CaF_2, and LiF, respectively. In Fig. 3, the curved surface was fitted and subtracted in order to examine the surface roughness. Interestingly, this procedure also reveals the scratches left by the abrasive particles during the polishing process, as thin layers of crystals are mechanically removed. Compared with the AFM technique, the white-light interferometer can examine a larger surface profile with a faster speed. However, it has relatively poor spatial resolution, especially for the lateral resolution due to the diffraction limit of the visible light microscope. Nevertheless, the vertical resolution is better than 1 nm in our homemade interferometer, which is sufficient for the purpose of this work. During the measurements, we first use low magnification settings to locate the cavity edge and then set it to 40× for final scanning, which covers an area up to 240 μm × 180 μm. One can observe that the scratches scattered on the rim surface are much lower in MgF_2 and CaF_2 [Figs. 3(a) and 3(b), resp.] than in LiF [Figs. 3(c)], thereby leading to intrinsic Q-factors that are an order of magnitude higher than in the LiF WGMR. The surface roughness profile of SrF_2 has already been published in [23], and it shares quantitative similarities with the ones of MgF_2 and CaF_2.

The dependence of Q-factors at 1550 nm on the roughness of these WGMRs is then plotted in Fig. 4. The protocol for obtaining a single point results from the repetition of the following sequence: (i) polishing the rim of the disk; (ii) measuring the surface roughness with the white-light interferometer; (iii) measuring the Q-factor. Each of these three procedures has to be repeated for each crystal under study, namely, MgF_2, CaF_2, and SrF_2. At this stage of our study, we have not considered LiF, due to its Q-factors being an order of magnitude lower than the other crystals. It should be noted that the polishing process is particularly time-consuming: several hours of polishing are required to shape a barium fluoride disk-resonator into an ultrahigh-Q WGM resonator [48], even though its hardness is particularly low, ∼3 on the mohs scale. Because of the lengthy polishing process, we could not obtain Q-factor data with the same roughness scale for the three crystals under consideration. This procedure also has two main methodological weaknesses, which can hardly be circumvented for a mm-size WGM resonator. The first one is that mm-size

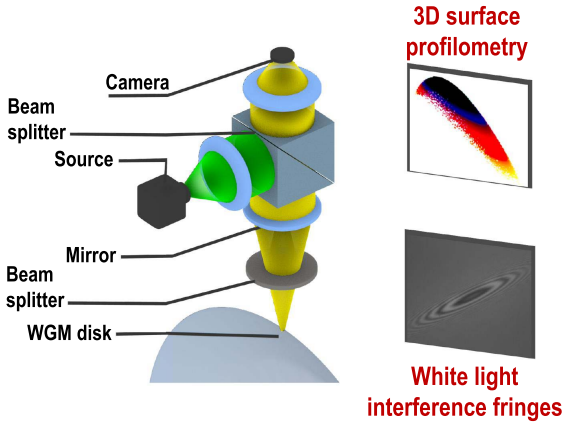

Fig. 1. Mirau-type interferometric microscope used to perform the 3D profilometry for surface roughness and the fringe pattern with white-light interferometry. This experimental setup allows us to determine the roughness of the WGMR surface with a vertical precision better than 1 nm.

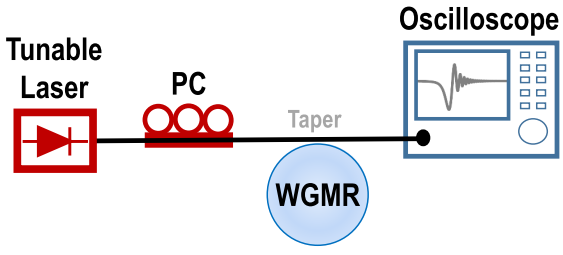

Fig. 2. Setup for the cavity-ring-down measurements of the Q-factors. The laser wavelength is $\lambda_0 \simeq 1550$ nm. PC, polarization controller; WGMR, whispering-gallery mode resonator. This experimental setup allows us to determine the intrinsic Q-factor of the resonators from $\sim 10^8$ and above.

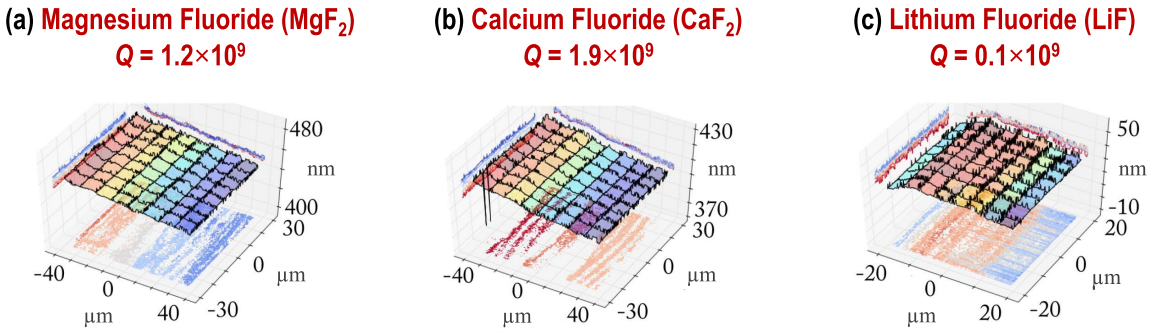

Fig. 3. Experimental surface roughness measurements for three different crystals. Note that the surface roughness of MgF_2 and CaF_2 is of the order of a nanometer, yielding $Q \sim 10^9$. The surface roughness of LiF is significantly higher and therefore leads to a quality factor that is an order of magnitude lower.

resonators are highly multimode, and it is difficult to ensure that we are addressing the same mode as the resonator is sequentially coupled and decoupled. Therefore, even though the highest Q-factor will have the tendency to be featured by the same mode, we are not absolutely certain that we are keeping track of that same mode at each polishing step. The second one arises from the fact that surface roughness is evaluated in a limited area of approximately ~100 μm × 100 μm and is not necessarily representative of the surface quality or roughness all along the rim. We therefore have to consider these two aspects as inherent sources of uncertainty in our experimental protocol.

Our experimental data sets are displayed in Fig. 4, using markers. The dependence of the Q-factors of these WGMRs with the surface roughness shows that, as expected, the Q-factor increases, as the surface roughness is decreased via the repetition of polishing steps with smaller abrasive particles. We find that a surface roughness smaller than 2 nm rms is required to achieve a Q-factor above a billion at 1550 nm for mm-size WGMRs. We have compared these experiments with two theoretical estimations of the surface scattering Q-factor available in the literature. The first one is the model derived by Vernooy *et al.* in [38], which can be explicitly written as (Model A)

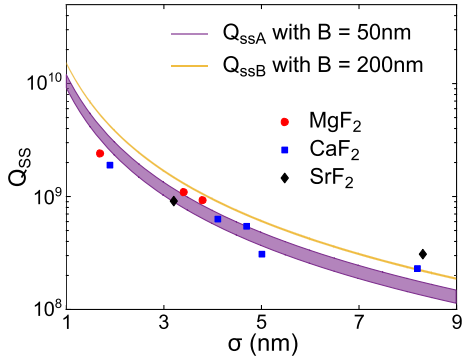

Fig. 4. Measured Q-factors as a function of surface roughness σ with MgF_2, CaF_2, and SrF_2 WGMRs (markers) and the estimated roughness-limited Q_{ss} from theoretical Eqs. (1) and (2) (shadow areas). Note that the shadow regions are given by the corresponding upper and lower curves corresponding to the lowest (MgF_2) and highest (SrF_2) refractive indices.

$$Q_{ssA} \simeq \frac{3n^2(n^2+2)^2}{(4\pi)^3(n^2-1)^{5/2}} \frac{\lambda^{7/2}D^{1/2}}{\sigma^2 B^2}, \tag{1}$$

where n is the refractive index of the host material, λ is the optical wavelength, and D is the diameter of the resonator, while σ and B are the rms roughness and its correlation length, respectively. The second model was proposed by Gorodetsky *et al.* [39] and is expressed as (Model B)

$$Q_{ssB} \simeq \frac{3\lambda^3 D}{16\pi^2 n\sigma^2 B^2}, \tag{2}$$

where the parameters are the same as in the first model.

The parameters for both models are experimentally accessible, except for the spatial correlation length B because of the limited lateral resolution of our profilometer. Therefore, for comparison between the experimental data and the theoretical estimations, we have considered B as a fitting parameter in Eqs. (1) and (2), respectively. However, it should be noted that, because of the point spread function of our objective lens, the correlation length B should be larger than the one obtained with an AFM. In consequence, using our experimental setup, B can be estimated to be in the range of few hundreds of nanometers, as discussed in [49]. Accordingly, the theoretical estimation of the Q-factors match the experimental data when we assume such large correlation length values ($B \gg \sigma$), in accordance with the characteristics of our interferometric measurement setup. The corresponding results are displayed in Fig. 4.

Conversely, if we had assumed $B \sim 1 - 10 \times \sigma$ (generally in the order of few nm) as is usually done in the literature, our experimental Q-factors would have been 1 or 2 orders of magnitude below the theoretical estimations. Our experimental data indicates that the rms surface roughness requirement for achieving a billion Q-factors tends to be 1–2 nm instead of 10–20 nm, as suggested by models A or B, when B and σ have the same order of magnitude. This large discrepancy has in fact already been previously reported. For example, Grudinin *et al.* reported in [50] a study where a CaF_2 WGM resonator with $D = 1.6$ mm and $\sigma = 0.33$ nm yielded a Q-factor of $\sim 10^9$, far below the estimated upper bound of $\sim 10^{12}$ using Model B and also far below the record Q-factor of $\sim 10^{11}$ at 1550 nm achieved in [3].

The fact that the parameter B seems to be larger than expected for models A and B could have multiple explanations, beyond the intrinsic differences between AFM and interferometric measurement techniques that have been highlighted

earlier. One can outline the fact that there is indeed a coupling between surface and volume losses during the high-speed polishing process, which is the source of a strong tangential stress at the inner periphery of the disk; this stress creates crystalline microdefects exactly in the mode volume where the intracavity field is propagating. Such microdefects can be relaxed using annealing methods, which permits to reach the highest Q-factors to this date [3]. Another effect that could lead to a dramatic increase of the parameter B is the multiscale nature of the surface roughness [49]; unlike the surface tension, which creates a homogeneous and isotropic surface roughness distribution in microspheres before solidification, the grinding and polishing method creates an inhomogeneous, anisotropic, and multiscale distribution of micro-scratches on the rim of the disk resonator. Finally, it is important to emphasize that, as σ is decreased and Q is accordingly increased, nonlinear intracavity scattering (such as Raman or Brillouin) starts to affect the photon lifetime in the resonator and contradict the initial hypothesis of surface-scattering-limited losses [51].

In conclusion, we used a homemade white-light interferometer to investigate the dependency of Q-factors with the surface roughness for mm-size WGM resonators. We have considered three different difluoride crystals as bulk materials; in all cases, we have found that a billion Q-factors at 1550 nm are achieved when the rms surface roughness has a nanometer order of magnitude. We have also compared our experimental data with theoretical estimations. This comparison enabled us to highlight a mismatch, which can be explained by the many physical constraints imposed by the mechanical grinding and polishing protocol. We expect that our work will contribute to a better understanding of the Q-factor limitations for mm-size WGM resonators, which are finding applications in a broad range of areas.

Funding. Centre National d'Etudes Spatiales (CNES); H2020 European Research Council (ERC) (278616, 632108); Labex ACTION.

REFERENCES

1. D. V. Strekalov, C. Marquardt, A. B. Matsko, H. G. L. Schwefel, and G. Leuchs, J. Opt. **18**, 123002 (2016).
2. G. Lin, A. Coillet, and Y. K. Chembo, Adv. Opt. Photon. **9**, 828 (2017).
3. A. A. Savchenkov, A. B. Matsko, V. S. Ilchenko, and L. Maleki, Opt. Express **15**, 6768 (2007).
4. V. Huet, A. Rasoloniaina, P. Guillemé, P. Rochard, P. Féron, M. Mortier, A. Levenson, K. Bencheikh, A. Yacomotti, and Y. Dumeige, Phys. Rev. Lett. **116**, 133902 (2016).
5. Y. K. Chembo, Nanophotonics **5**, 214 (2016).
6. A. Chiasera, Y. Dumeige, P. Feron, M. Ferrari, Y. Jestin, G. Nunzi Conti, S. Pelli, S. Soria, and G. C. Righini, Laser Photon. Rev. **4**, 457 (2010).
7. V. S. Ilchenko, A. A. Savchenkov, A. B. Matsko, and L. Maleki, Phys. Rev. Lett. **92**, 043903 (2004).
8. J. U. Fürst, D. V. Strekalov, D. Elser, M. Lassen, U. L. Andersen, C. Marquardt, and G. Leuchs, Phys. Rev. Lett. **104**, 153901 (2010).
9. T. Beckmann, H. Linnenbank, H. Steigerwald, B. Sturman, D. Haertle, K. Buse, and I. Breunig, Phys. Rev. Lett. **106**, 143903 (2011).
10. Y. Pan, G. Lin, S. Diallo, X. Zhang, and Y. K. Chembo, IEEE Photon. J. **9**, 2700608 (2017).
11. G. Lin, J. U. Fürst, D. V. Strekalov, and N. Yu, Appl. Phys. Lett. **103**, 181107 (2013).
12. G. Lin and N. Yu, Opt. Express **22**, 557 (2014).
13. J. U. Fürst, K. Buse, I. Breunig, P. Becker, J. Liebertz, and L. Bohatý, Opt. Lett. **40**, 1932 (2015).
14. S.-K. Meisenheimer, J. U. Fürst, K. Buse, and I. Breunig, Optica **4**, 189 (2017).
15. K. Volyanskiy, P. Salzenstein, H. Tavernier, M. Pogurmirskiy, Y. K. Chembo, and L. Larger, Opt. Express **18**, 22358 (2010).
16. S. B. Papp and S. A. Diddams, Phys. Rev. A **84**, 053833 (2011).
17. A. A. Savchenkov, A. B. Matsko, D. Strekalov, M. Mohageg, V. S. Ilchenko, and L. Maleki, Phys. Rev. Lett. **93**, 243905 (2004).
18. I. S. Grudinin, A. B. Matsko, and L. Maleki, Phys. Rev. Lett. **102**, 043902 (2009).
19. A. Chen-Jinnai, T. Kato, S. Fujii, T. Nagano, T. Kobatake, and T. Tanabe, Opt. Express **24**, 26322 (2016).
20. W. Liang, A. A. Savchenkov, A. B. Matsko, V. S. Ilchenko, D. Seidel, and L. Maleki, Opt. Lett. **36**, 2290 (2011).
21. G. Lin, S. Diallo, K. Saleh, R. Martinenghi, J.-C. Beugnot, T. Sylvestre, and Y. K. Chembo, Appl. Phys. Lett. **105**, 231103 (2014).
22. Y. K. Chembo, I. S. Grudinin, and N. Yu, Phys. Rev. A **92**, 043818 (2015).
23. R. Henriet, G. Lin, A. Coillet, M. Jacquot, L. Furfaro, L. Larger, and Y. K. Chembo, Opt. Lett. **40**, 1567 (2015).
24. S. Diallo, G. Lin, R. Martinenghi, L. Furfaro, M. Jacquot, and Y. K. Chembo, IEEE Photon. Technol. Lett. **28**, 955 (2016).
25. G. Lin and Y. K. Chembo, Opt. Lett. **41**, 3718 (2016).
26. G. Lin, S. Diallo, J. M. Dudley, and Y. K. Chembo, Opt. Express **24**, 14880 (2016).
27. M. R. Foreman, J. D. Swaim, and F. Vollmer, Adv. Opt. Photon. **7**, 168 (2015).
28. Y. Li, O. V. Svitelskiy, A. V. Maslov, D. Carnegie, E. Rafailov, and V. N. Astratov, Light Sci. Appl. **2**, e64 (2013).
29. Y. Li, A. V. Maslov, N. I. Limberopoulos, A. M. Urbas, and V. N. Astratov, Laser Photon. Rev. **9**, 263 (2015).
30. Y. Li, F. Abolmaali, K. W. Allen, N. I. Limberopoulos, A. Urbas, Y. Rakovich, A. V. Maslov, and V. N. Astratov, Laser Photon. Rev. **11**, 1600278 (2017).
31. J. Li, M.-G. Suh, and K. Vahala, Optica **4**, 346 (2017).
32. W. Liang, V. S. Ilchenko, A. A. Savchenkov, E. Dale, D. Eliyahu, A. B. Matsko, and L. Maleki, Optica **4**, 114 (2017).
33. Y. K. Chembo, Phys. Rev. A **93**, 033820 (2016).
34. K. Saleh, R. Henriet, S. Diallo, G. Lin, R. Martinenghi, I. V. Balakireva, P. Salzenstein, A. Coillet, and Y. K. Chembo, Opt. Express **22**, 32158 (2014).
35. K. Saleh, G. Lin, and Y. K. Chembo, IEEE Photon. J. **7**, 5500111 (2015).
36. V. Braginsky, M. Gorodetsky, and V. Ilchenko, Phys. Lett. A **137**, 393 (1989).
37. M. L. Gorodetsky, A. A. Savchenkov, and V. S. Ilchenko, Opt. Lett. **21**, 453 (1996).
38. D. W. Vernooy, V. S. Ilchenko, H. Mabuchi, E. W. Streed, and H. J. Kimble, Opt. Lett. **23**, 247 (1998).
39. M. L. Gorodetsky, A. D. Pryamikov, and V. S. Ilchenko, J. Opt. Soc. Am. B **17**, 1051 (2000).
40. G. Righini, Y. Dumeige, P. Féron, M. Ferrari, G. Nunzi Conti, D. Ristic, and S. Soria, Riv. Nuovo Cimento Soc. Ital. Fis. **34**, 435 (2011).
41. L. Maleki, Nat. Photonics **5**, 728 (2011).
42. A. Coillet, R. Henriet, K. P. Huy, M. Jacquot, L. Furfaro, I. Balakireva, L. Larger, and Y. K. Chembo, J. Visualized Exp. **78**, e50423 (2013).
43. P. J. Caber, Appl. Opt. **32**, 3438 (1993).
44. P. de Groot and L. Deck, J. Mod. Opt. **42**, 389 (1995).
45. P. Sandoz, J. Mod. Opt. **43**, 1545 (1996).
46. P. Sandoz, R. Devillers, and A. Plata, J. Mod. Opt. **44**, 519 (1997).
47. Y. Dumeige, S. Trebaol, L. Ghişa, T. K. N. Nguyen, H. Tavernier, and P. Féron, J. Opt. Soc. Am. B **25**, 2073 (2008).
48. G. Lin, S. Diallo, R. Henriet, M. Jacquot, and Y. K. Chembo, Opt. Lett. **39**, 6009 (2014).
49. B. Bhushan, *Modern Tribology Handbook* (CRC Press, 2000).
50. I. S. Grudinin, A. B. Matsko, A. A. Savchenkov, D. Strekalov, V. S. Ilchenko, and L. Maleki, Opt. Commun. **265**, 33 (2006).
51. I. S. Grudinin, A. B. Matsko, and L. Maleki, Opt. Express **15**, 3390 (2007).